JOURNAL OF MATERIALS SCIENCE 26 (1991) 5623–5630

Isobaric sections of the aluminium phase field in the Al–Ge phase diagram at high pressures up to 2.6 GPa

YORITOSHI MINAMINO, TOSHIMI YAMANE, HIDEKI ARAKI, TOMOHIKO ADACHI, YAN-SHENG KANG
Department of Materials Science and Engineering, Osaka University, 2-1 Yamadaoka, Suita, Osaka 565, Japan

YOSHINARI MIYAMOTO, TAIRA OKAMOTO
Institute of Scientific and Industrial Research, Osaka University, 8-1 Mihogaoka, Ibaraki, Osaka 567, Japan

The isobaric sections of the aluminium phase field in the Al–Ge system have been obtained experimentally at 0.1 MPa, 2.2 and 2.6 GPa. The solidus and solid solubility lines of the aluminium phase were determined by electron probe microanalysis of alloys quenched after equilibration at known temperatures and pressures. The aluminium phase field of aluminium was observed to expand with increasing pressure. This result was compared with the phase diagrams calculated on the basis of thermodynamic and volumetric data at 0.1 MPa. The calculations are in qualitative agreement with the experimental results.

1. Introduction

Large hydrostatic pressures applied to materials can induce a change in both the phase equilibria and the kinetics of the approach to equilibrium [1]. Knowledge of the composition–temperature–pressure (*C–T–P*) phase relation is essential to the treatment of materials under high pressures, such as hot-isostatic pressing, synthesis, and casting under high pressures. Therefore, it is worthwhile to elucidate the effect of high pressure on the phase equilibria experimentally, and to compare the observed results with predicted pressure effects derived on the basis of known thermodynamic and volumetric data at atmospheric pressure.

According to the binary alloy phase diagrams (BAPD), aluminium and germanium form a simple eutectic system with the eutectic point at approximately 28.4 at % Ge, 693 K and 0.1 MPa [2]. This system exhibits only three phases: the aluminium phase (Al), germanium phase (Ge) and liquid phase (L). The liquidus line in the aluminium-rich part is well-known, but the solidus line has not yet been reported. Limited data on solid solubility have been presented [3–5]. Its maximum is vague but seems to be about 2–3 at % Ge at the eutectic temperature [2, 4]. The melting curves of aluminium and germanium at high pressures were studied by several researchers, and their results were collected and presented in the *T–P* phase diagrams by Tonkov [6]. Clark and Pistorius [7] investigated the eutectic temperature at high pressures in detail using the DTA method. However, no research work on the aluminium fields at high pressures has been reported except for that by Banova *et al.* [5]. Banova *et al.* measured the lattice parameters of solid solutions of Al–Ge alloys annealed at 673 K and 2.0 GPa, and reported only the value of solid solubility of 4.8 at % Ge in the aluminium phase. They also calculated the Al–Ge phase diagrams at 0.1 MPa and 2.0 GPa on the basis of the ideal solution model and the volumetric data, taking no account of their pressure and temperature dependences. There was a difference of 20–48 K in the melting points of aluminium and germanium at 2.0 GPa between their calculated results and the experimental data compiled by Tonkov. In addition, Kingon and Clark [8] pointed out that the eutectic temperature calculated by Banova *et al.* deviated from Clark and Pistourius's results [7] as pressure increased.

The aims of this work were: (1) to determine the solidus and solid solubility lines in the aluminium-rich part of the Al–Ge system at pressures of 0.1 MPa, 2.2 and 2.6 GPa using the process of electron probe microanalysis of alloys quenched after equilibration at known temperatures and pressures; (2) to revise the calculations of the phase diagrams at high pressures using the regular solution model and volumetric data, taking account of their temperature and pressure dependences; and (3) to compare the observed results for the high pressures with the calculated phase diagrams.

2. Experimental procedure

The alloys of 0.77, 1.17, 1.91, 2.81, 4.10 and 8.40 at % Ge were prepared by melting together appropriate quantities of aluminium (99.993%) and germanium

0022–2461/91 $03.00 + .12

(99.9999%) in alumina crucibles in an electric furnace under atmospheric conditions. These alloy ingots were homogenized for 346 ks at 673–823 K again under atmospheric conditions. The cylindrical alloys, 5 mm high, 4 mm diameter, were made of these alloys by a lathe and a cutter.

Each of the cylindrical alloys of 1.91, 2.81 and 4.10 at % Ge was sealed into silica tubes filled with argon gas, and these sealed silica tubes were annealed at 633–893 K for 7.2–86.4 ks in the electric furnace. The annealing temperatures were controlled to within ± 0.5 K. The argon gas pressure in the sealed silica tubes at the annealing temperatures was 0.1 MPa. On removal from the furnace, the silica tubes were immediately broken open in ice–water to facilitate rapid cooling of the cylindrical alloys with the object of preserving the concentration of the phases at the annealing temperatures.

For treatments at high pressures, each of the cylindrical alloys of 2.81, 4.10 and 8.40 at % Ge was inserted into the cubical cell, as shown in Fig. 1. The cell consists of a boron nitride (BN) capsule, a graphite tube, a thermocouple (Pt/Pt–13% Rh), a cubical block of pyrophyllite ($Al_2Si_4O_{10}(OH)_2$), and two copper caps. The BN capsule is thermally stable and has the proper lubricity. The graphite tube is the heater. The pyrophyllite fulfils the functions as a pressure medium and is also self-gasketing. The high-pressure equipment consists of a 12 MN press machine and an apparatus with six anvils of tungsten carbide (WC). The apparatus is designed to convert a uni-press generated by the 12 MN press machine into six equal presses from the six anvils. The six anvils compress the cubical cell and result in a hydrostatic high pressure on the cylindrical alloy. The alloys, under high pressure up to 2.6 GPa, were heated to annealing temperatures of 653–1003 K within about 60 s and held for annealing times of 3.6–50.4 ks. The annealing temperatures were controlled to within ± 2 K. After annealing at high pressures, the alloys were cooled to room temperature within about 20 s, and then the pressure was released. The initial cooling rate was over 70 K s^{-1}. After annealing, the annealed alloys were removed from the cells. The calibration of temperature was carried out using a technic similar to Hanneman and Strong's method [9], and the pressure was calibrated through the measurement of the transition of bismuth I to II (2.55 GPa at room temperature) and II to III (2.7 GPa at room temperature). The pressures, temperatures and times are listed in Table I.

These annealed alloys were mounted in synthetic resin, ground and metallographically polished. They were analysed using an electron probe microanalyser (EPMA) to determine germanium concentrations in the aluminium phase. The characteristic X-ray intensity of germanium (K_α line) was measured using a wavelength dispersive X-ray spectrometer (WDX) with an analysing crystal of LiF, and converted to concentration using the following equation, which was presented by Ziebold *et al.* [10]

$$(1 - I_{Ge}^{WDX})/I_{Ge}^{WDX} = K(1 - X_{Ge})/X_{Ge} \quad (1)$$

where I_{Ge}^{WDX} is the relative intensity of the germanium K_α line, X_{Ge} the weight fraction, and K the conversion parameter, which was determined to be 0.929 through calibration experiments using pure aluminium, pure germanium and their alloys as standards. The microstructures of the Al–Ge alloys were observed using a scanning electron microscope (SEM) with an energy dispersive X-ray spectrometer (EDX).

3. Calculation of the phase diagram at high pressure

The free energy of A-phase at a molar fraction X, a temperature T and a pressure of 0 is presented by the regular solution model [11]

$$G^A(X, T, 0) = {}^oG_a^A(T)X_a^A + {}^oG_b^A(T)X_b^A + RT\{X_a^A \ln(X_a^A) + X_b^A \ln(X_b^A)\} + {}^{ex}G^A(X, T) \quad (2)$$

where subscripts a and b are the atomic species, R is the gas constant, ${}^oG^A(T)$ the free energy of a pure element in the A-phase, and ${}^{ex}G^A(X, T)$ the excess free energy. According to the regular solution model, ${}^{ex}G^A(X, T)$ is given by

$${}^{ex}G^A(X, T) = Q_{ab}^A(X, T)X_a^A X_b^A \quad (3)$$

where $Q_{ab}^A(X, T)$ is the interaction parameter of the A-phase. Table II presents the thermodynamic values, quoted from the literature [12–14], used to calculate the phase diagram of the Al–Ge system at 0.1 MPa.

The free energies, $G(X, T, P)$, at high pressures of P, which are used to calculate the phase diagram at high pressures, can be evaluated by the following equation [15]

$$G^A(X, T, P) = G^A(X, T, 0) + \int_0^P V^A(X, T, P)\,dP \quad (4)$$

where $V^A(X, T, P)$ is the molar volume of A-phase. The molar volumes are assumed to have the following form for simplicity

$$V^A(X, T, P) = {}^oV_a^A(T, P)X_a^A + {}^oV_b^A(T, P)X_b^A \quad (5)$$

$${}^oV_i^A(T, P) = {}^oV_i^A(T_0^A, 0)\{1 + {}^TK_i^A(T - T_0^A)\} \times (1 - {}^PK_i^A P) \quad (6)$$

(i = a or b)

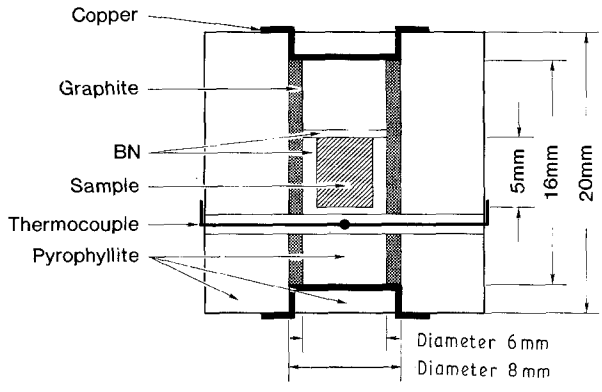

Figure 1 Cubic cell for the high-pressure annealing.

TABLE I Temperatures, pressures and times of annealing, and the germanium concentrations of the aluminium phases

Alloy (at % Ge)	Pressure (MPa)	Pressure (GPa)	Temperature (K)	Time (ks)	Concentration (at % Ge)
1.91	0.1		893	7.2	0.78
2.81	0.1		873	7.2	1.04
2.81	0.1		853	7.2	1.28
2.81	0.1		833	7.2	1.39
4.10	0.1		813	7.2	1.80
4.10	0.1		803	7.2	1.91
4.10	0.1		793	7.2	1.98
4.10	0.1		773	7.2	2.08
4.10	0.1		763	7.2	2.21
4.10	0.1		753	14.4	2.29
4.10	0.1		743	7.2	2.28
4.10	0.1		733	14.4	2.43
4.10	0.1		723	14.4	2.42
4.10	0.1		713	14.4	2.59
4.10	0.1		703	14.4	2.58
4.10	0.1		693	28.8	2.52
2.81	0.1		683	86.4	2.13
4.10	0.1		673	28.8	1.84
2.81	0.1		653	57.6	1.55
2.81	0.1		633	57.6	1.21
2.81		2.2	1003	3.6	1.65
4.10		2.2	963	3.6	2.35
4.10		2.2	923	3.6	2.53
4.10		2.2	883	3.6	3.11
8.40		2.2	843	3.6	4.20
8.40		2.2	803	7.2	4.33
8.40		2.2	763	7.2	4.93
8.40		2.2	743	7.2	4.91
8.40		2.2	713	14.4	5.58
8.40		2.2	693	28.8	6.44
4.10		2.2	673	28.8	3.86
4.10		2.2	653	50.4	2.60
4.10		2.6	1003	3.6	2.09
4.10		2.6	963	3.6	2.89
4.10		2.6	923	3.6	4.06
8.40		2.6	883	3.6	4.67
8.40		2.6	843	3.6	5.42
8.40		2.6	803	7.2	5.35
8.40		2.6	763	7.2	5.97
8.40		2.6	743	7.2	6.42
8.40		2.6	713	14.4	6.56
8.40		2.6	693	28.8	6.76
8.40		2.6	673	28.8	5.50
4.10		2.6	653	50.4	3.34

where ${}^{\circ}V^{A}$ is the molar volume of A-phase of pure element, ${}^{T}K^{A}$ the constant of thermal expansion, T_0^A the standard temperature and ${}^{P}K^{A}$ the constant of compressibility. The values of the molar volumes and constants are summarized in Table III, where D denotes the diamond cubic structure, fcc the face centred cubic structure, and L the liquid state. Most of those values are quoted from the literature and derived from lattice parameter data [16–19]. Unfortunately, the values for V_{Al}^{D} and V_{Ge}^{fcc} are unavailable because the D-aluminium and fcc-germanium phases do not exist in the equilibrium state at 0.1 MPa. It was therefore necessary to make an indirect estimate and some assumptions for the volumes of these phases. The value of ${}^{\circ}V_{Ge}^{fcc}$ was evaluated by an extrapolation of the molar volumes of the fcc-aluminium phase to pure germanium. The value of ${}^{\circ}V_{Al}^{D}$ was assumed to have the molar volume of $13 \times 10^{-6}\ m^3\ mol^{-1}$. This value is thought to be reasonable as compared with the other molar volumes of fcc-aluminium, fcc-silicon, D-silicon and L. The thermal expansion and compressibility of the fcc-germanium and D-aluminium phases were assumed to have the same values as the fcc-aluminium and D-germanium phases, respectively.

When the A-phase is in equilibrium with the B-phase, the chemical potentials of both phases, which are derived from Equation 4, are equal to each other [11]

$$\mu_a^A(X, T, P) = \mu_a^B(X, T, P) \quad (7)$$

$$\mu_b^A(X, T, P) = \mu_b^B(X, T, P) \quad (8)$$

where μ is the chemical potential. The solution of Equations 7 and 8 was obtained by Newton–Raphson's method in order to calculate the equilibrium concentrations of the A- and B-phases for construction of the phase diagram [20].

TABLE II The thermodynamic values used in this work to calculate the phase diagrams of the Al–Ge system [12–14]

Phase stability	(J mol^{-1})
${}^{\circ}G^{fcc}_{Al}(T) - {}^{\circ}G^{L}_{Al}(T)$	$-10711.0 + 11.506T$
${}^{\circ}G^{D}_{Al}(T) - {}^{\circ}G^{L}_{Al}(T)$	$0 + 30.0T$
${}^{\circ}G^{fcc}_{Ge}(T) - {}^{\circ}G^{L}_{Ge}(T)$	$5021.0 + 8.368T$
${}^{\circ}G^{D}_{Ge}(T) - {}^{\circ}G^{L}_{Ge}(T)$	$-36944.7 + 30.522T$
Phases	${}^{ex}H$ [(J mol^{-1})/$X_{Al}X_{Ge}$]
L	$-11482 - 418(1 - 2X_{Ge}) + 3035(X^2_{Ge} - X_{Ge} + 1/6)$
fcc	$540 - 11000(1 - 2X_{Ge})$
D	12000
Phases	${}^{ex}S$ [(J mol^{-1})/$X_{Al}X_{Ge}$]
L	$4.732 + 0.335(1 - 2X_{Ge}) + 1.55(X^2_{Ge} - X_{Ge} + 1/6)$
fcc	0
D	12

4. Results and discussion

Fig. 2a–c show the microstructures of Al–4.10 at % Ge alloys annealed under conditions of (a) at 673 K for 346 ks under 0.1 MPa, (b) at 673 K for 28.8 ks under 0.1 MPa after (a), and (c) at 673 K for 28.8 ks under 2.2 GPa after (a), respectively. The intensities of characteristic X-rays of germanium in the aluminium phase obtained using EDX, I^{EDX}_{Ge}, are also presented in Fig. 2. In Fig. 2a, many particles uniformly precipitate in the aluminium phase of the alloy annealed under the conditions of (a). The electron probe microanalysis showed these particles to be the germanium phase. The existence of the germanium phase particles indicates that the concentration of 4.10 at % Ge is over the solid solubility of germanium in the aluminium phase at 673 K and 0.1 MPa.

The effect of high pressure on the germanium solubility in the aluminium phase is strikingly demonstrated by a comparison of Fig. 2b and c. A structure similar to that of Fig. 2a was observed in the alloy annealed under the conditions of (b), as seen in Fig. 2b. The germanium phase retains much the same size and number of particles as it had before being additionally annealed. Furthermore, the germanium concentrations of the aluminium phase in alloys annealed under the conditions of (a) and (b) are apparently almost equal as indicated by the I^{EDX}_{Ge}. On the other hand, as shown in Fig. 2c, additional annealing at 2.2 GPa allows most of the germanium phase particles to

TABLE III The values of molar volumes and constants of thermal expansion and compressibility of the phases in the Al–Ge system

Element (i)	Phase (A)	${}^{\circ}V^{A}_{i}$ (10^{-6}m^3 mol^{-1})	${}^{T}K^{A}_{i}$ (10^{-5} K^{-1})	${}^{P}K^{A}_{i}$ (10^{-11} Pa^{-1})	T^{A}_{o} (K)
Al	L	11.4 [19]	10.7 [19]	2.14 [17]	933
	fcc	9.91 [16]	10.7 [16]	1.68 [18]	300
	D	13.0[a]	2.25[b]	1.32[b]	293
Ge	L	13.2 [17]	8.9 [17]	1.83 [17]	1232
	fcc	11.2[c]	10.7[d]	1.68[d]	300
	D	13.63 [16]	2.25 [16]	1.32 [18]	293

[a] Value which D-aluminium is assumed to have.
[b] Same values as those for D-germanium.
[c] Value evaluated by extrapolation from molar volumes of fcc-aluminium to that of fcc-germanium.
[d] Same values as those for fcc-aluminium.

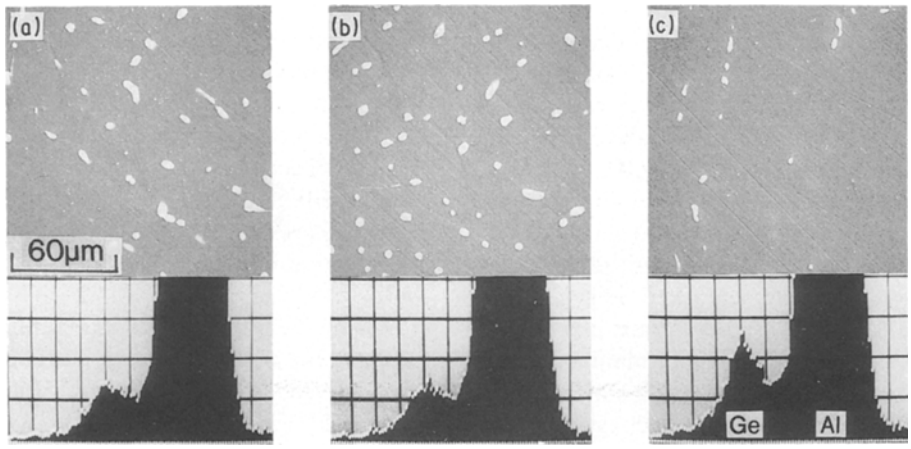

Figure 2 Structures and I^{EDX}_{Ge} of the Al–4.10 at % Ge alloys annealed at (a) 673 K and 0.1 MPa for 346 ks, (b) 673 K and 0.1 MPa for 28.8 ks after (a), and (c) 673 K and 2.2 GPa for 28.8 ks after (a).

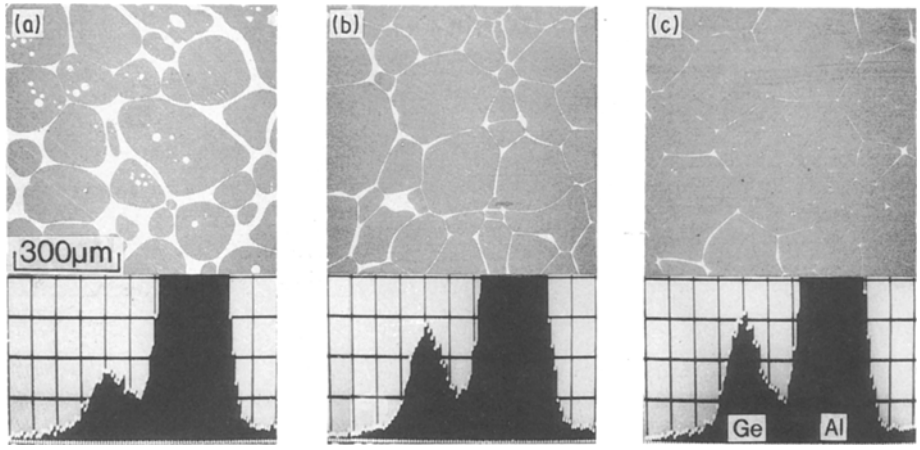

Figure 3 Structures and I_{Ge}^{EDX} of the Al–8.40 at % Ge alloys annealed at 713 K for 14.4 ks at pressures of (a) 0.1 MPa, (b) 2.2 GPa and (c) 2.6 GPa.

dissolve into the aluminium phase and thereby causes the germanium concentration of the aluminium phase to increase by about twice compared to those at 0.1 MPa. This indicates that the solid solubility line is shifted to a higher concentration of germanium by high pressure.

Fig. 3a–c show the results for the Al–8.40 at % Ge alloys annealed at 713 K under 0.1 MPa, 2.2 and 2.6 GPa, respectively. Evidence of partial melting was observed in these alloys annealed at all the pressures, but it was noticed that the volume fraction of the liquid phase decreases with increasing pressure while the I_{Ge}^{EDX} in the aluminium phase increases. The decrease in the volume fraction of the liquid phase suggests that a shift of the liquidus line and the eutectic point to a higher concentration of germanium occurs at high pressures.

Fig. 4a and b show the results for the Al–4.10 at % Ge alloys annealed at 763 K under 0.1 MPa and 2.2 GPa, respectively. In Fig. 4a a partially melted structure was observed in the alloy annealed at 763 K and 0.1 MPa. At this temperature and pressure the 4.10 at % Ge alloy exists in the two-phase field of the liquid and the aluminium phases. In contrast, as shown in Fig. 4b, only the aluminium phase was observed in the alloy annealed at 2.2 GPa. Therefore, the germanium over 4.10 at % Ge can be dissolved in the aluminium phase at 2.2 GPa. In fact, the I_{Ge}^{EDX} of the structure formed at 2.2 GPa (in Fig. 3b) is twice as large as that at 0.1 MPa.

Fig. 5a and b show the results for the Al–4.10 at % Ge alloys annealed at the higher temperature of 923 K under 0.1 MPa and 2.2 GPa, respectively. As shown in Fig. 5a, the alloy annealed at 923 K and 0.1 MPa exhibits the fine network structure, which indicates that the alloy had been completely melted. This structure is produced when the complete melt is quenched because the solidification of the primary crystals of the aluminium phase proceeds first, and then the eutectic reaction takes place in the liquid phase around the large number of primary crystals already formed. At 0.1 MPa, the temperature of 923 K is high enough to melt the 4.10 at % Ge alloy completely. On the other hand, the structure of partial melting was observed in the alloy annealed at 2.2 GPa and 923 K as shown in Fig. 5b. Thus, even at 923 K, this alloy under 2.2 GPa remains in the two-phase region of the liquid and the aluminium phases. From the above observations, it follows that the high pressure causes the solidus and solubility lines to shift to a higher concentration and temperature, sufficient to bring about a change in the microstructure as opposed to the situation at 0.1 MPa.

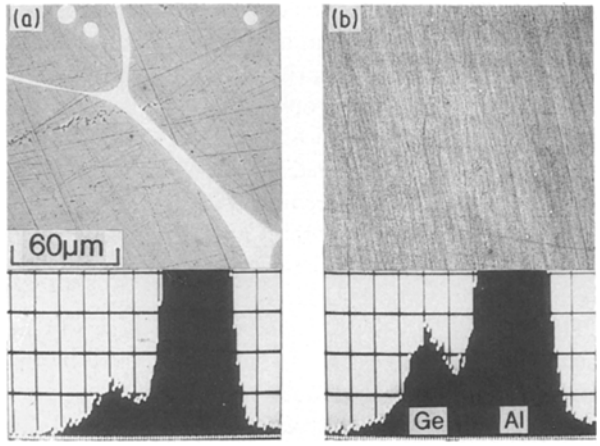

Figure 4 Structures and I_{Ge}^{EDX} of the Al–4.10 at % Ge alloys annealed at 763 K for 7.2 ks at (a) 0.1 MPa and (b) 2.2 GPa.

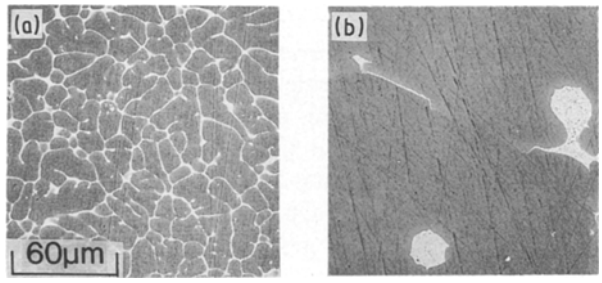

Figure 5 Structures of the Al–4.10 at % Ge alloys annealed at 923 K for 3.6 ks at (a) 0.1 MPa and (b) 2.2 GPa.

The germanium concentrations in the aluminium phase at 0.1 MPa, 2.2 and 2.6 GPa were determined by electron probe microanalysis using the WDX method. Their concentrations are listed in Table I and

plotted in Figs 6–8 together with the calculated lines for the same pressures. The pressure dependence of the melting points of aluminium and germanium were reported to be 65 and $-33\ \mathrm{K\,GPa^{-1}}$ [6], respectively. From these dependences, the melting points of aluminium and germanium at each of the pressures were evaluated and included in the figures. It is apparent from the sequence of isobaric sections presented in Figs 6–8 that the application of high pressure expands the aluminium phase field but causes very small changes in the eutectic temperature.

As shown in Fig. 6, the experimental solidus line at 0.1 MPa is not straight, but convex. According to the BAPD [2], the Al–Ga and Al–Li systems have similar convex solidus lines. The solid solubility line determined in this work is in good agreement with the data points reported by Stoehr and Klemm [4] and Caywood [3], with Banova *et al.* [5] being the only exception. The point of intersection of the solidus and solubility lines suggests that the eutectic point exists at 699 K. This value is nearly equal to the eutectic temperatures of 693 K proposed by the BAPD, and 697 K proposed by Stoehr and Klemm [4]. The maximum solubility determined in this work is 2.6 at % Ge, which is in good agreement with the value of 2.8 at% Ge suggested by Stoehr and Klemm [4], but somewhat high in comparison with the value of 2 at% Ge suggested by the BAPD.

The lines at 0.1 MPa, calculated on basis of the thermodynamic values [12–14] in Table II, exhibit the maximum solubility at about 4 at % Ge in the aluminium phase, the eutectic point at about 27 at % Ge and 700 K, and the solid solubility at about 1 at % Al in the germanium phase. A satisfactory agreement was found between the calculated and experimental solidus lines above 800 K in the aluminium-rich part of the Al–Ge system. However, below 800 K the calculated lines deviate from the experimental lines by about 1.5 at % Ge. This overestimation of the calculated lines affects the calculation results of phase diagrams at high pressures as is mentioned later.

As shown in Figs 7 and 8, the experimental solidus lines at pressures of 2.2 and 2.6 GPa have a curvature similar to that at 0.1 MPa, but shift progressively to a higher concentration of germanium with increasing pressure. The experimental solid solubility lines also shift to a higher concentration. The value of 4.8 at % Ge at 673 K and 2.0 GPa reported by Banova *et al.* [5] is slightly higher than the present results at 2.2 GPa. The maximum solubility at 2.6 GPa is about three times larger than that at 0.1 MPa. The eutectic temperatures of 704 K at 2.2 GPa and 702 K at 2.6 GPa are suggested from the points of intersection of solidus and solubility curves of this work. These values at 2.2 and 2.6 GPa are higher by 5 and 3 K, respectively, when compared to the value at 0.1 MPa. Clark and Pistorious [7] measured the eutectic points at high pressures using the DTA method. They reported that the eutectic temperature increases slightly with pressure to 1.39 GPa and then falls with the further pressure increase. From their data, the increments in the eutectic temperatures when the pressure increase from 0.1 MPa to 2.2 and 2.6 GPa are evaluated to be 3.4 and 1.3 K, respectively. The present increment in eutectic temperatures caused by high pressure are consistent with the results reported by Clark and Pistorious [7].

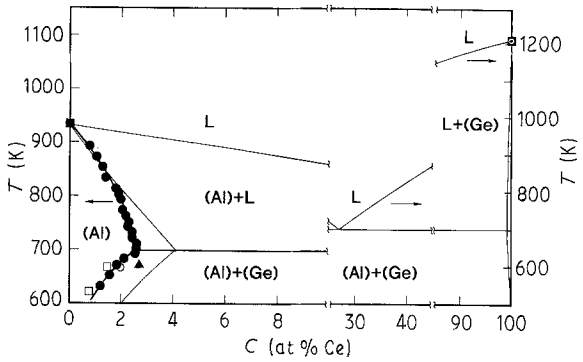

Figure 6 Isobaric section of the Al–Ge phase diagram at 0.1 MPa. (●) Present work, (▲) [5, 6], (○) [4], (□) [3].

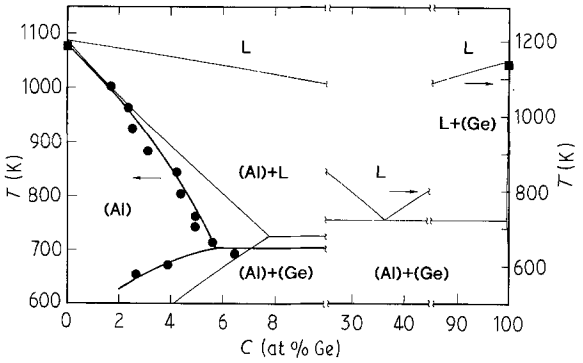

Figure 7 Isobaric section of the Al–Ge phase diagram at 2.2 GPa. (●) Present work, (■) [6].

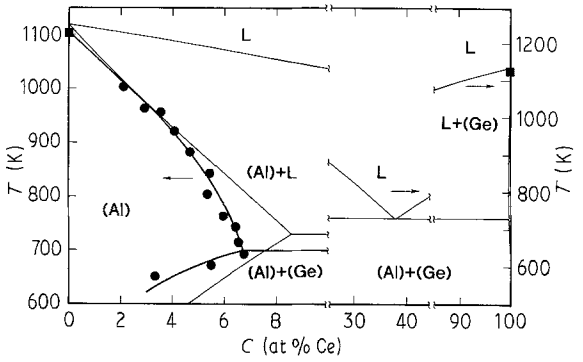

Figure 8 Isobaric section of the Al–Ge phase diagram at 2.6 GPa. (●) Present work, (■) [6].

The lines at 2.2 and 2.6 GPa calculated on the basis of the thermodynamic data for 0.1 MPa in Table II and the volumetric data for 0.1 MPa in Table III exhibit the following changes in phase equilibriums when the pressures is increased from 0.1 MPa: an increase in the melting point of aluminium; a decrease in the melting point of germanium; a shift of the eutectic point toward a higher temperature and concentration of germanium; an expansion of the aluminium phase; and an contraction of the germanium

phase. The calculated melting points of pure aluminium and germanium at high pressures are in good agreement with the experimental results [6]. The calculated shift of the eutectic point is consistent with the experimental suggestion as mentioned in discussion of Fig. 3. The calculated solidus lines are also in good agreement with the experimental lines from the melting point of aluminium down to about 800 K. However, below about 800 K the calculated lines deviate from the experimental lines, and the overestimation for the aluminium phase fields at high pressures retains the same magnitude of about 1.5 at % Ge observed at 0.1 MPa.

The cause of the overestimations is thought to lie in the estimations of free energies for the phases: the thermodynamic and volumetric terms of Equation 4. In order to evaluate the volumetric term, necessary to calculate the increment of free energy caused by the application of high pressure, Equation 6, which consists of three factors – the molar volume of a pure element, and its linear pressure and temperature dependences – was used for simplification. The form of Equation 5 represents the compositional proportionality of molar volume, that is, it ignores the excess term of molar volume. The volumetric data for the fcc-germanium and D-aluminium phases necessitates some assumptions in evaluation because of the non-existence of these phases under the usual conditions, as mentioned above. It is possible that these simplifications and assumptions may induce the over- or underestimations in the calculation for the high pressures. If the error in volumetric data was appreciable, then the over- or underestimation caused by that error in volumetric data becomes larger and more serious with increasing pressure because the increment of free energy caused by application of high pressure would play a more important role at higher pressures.

With regard to the thermodynamic term of Equation 4, according to Murray [12], Ansara *et al.* [13] has analysed the thermodynamic data of the liquid phase at 0.1 MPa derived from the most recent measurements, and calculated the liquidus line at 0.1 MPa accurately. Furthermore, combining with these data of the liquid phase, they derived the thermodynamic data of the solid aluminium phase from the phase diagram at 0.1 MPa which had an experimental uncertainty in the aluminium phase field. Therefore, their calculations of the phase diagram overestimate the experimental results of the solubility of germanium in the aluminium phase by about 2.5 at % Ge. Subsequently, Murray [12] performed a further readjustment of the fcc excess term to improve the calculation of the phase diagram at 0.1 MPa. However, those overestimations still remain at about 1.5 at % Ge.

In the present calculations which are performed on the basis of their thermodynamic data listed in Table II and the volumetric data listed in Table III, the magnitude of about 1.5 at % Ge overestimation stays constant for each pressure up to 2.6 GPa. In addition, good reproduction of the melting points and solidus line above 800 K is also obtained at high pressures. It follows, then, that no serious error exists in the volumetric data, and therefore the prime source of the overestimations of the phase diagrams at high pressures must lie in the thermodynamic data at 0.1 MPa. Further improvement in the calculations for the phase diagrams at high pressures will require more accurate thermodynamic data at 0.1 MPa, especially for the interaction parameter. However, although there are overestimations for each of the pressures mentioned above, the current calculation yields a prediction of the effect of high pressure on the phase equilibria sufficient to assess the phase diagram at high pressures.

The change in the phase equilibria caused by high pressure is closely related to the volumetric values of the phases. As the general rule [21], the application of high pressure may be expected to favour the denser phase and higher coordination because the thermodynamically stable phase has the minimum amount of Gibbs free energy, $G = U - TS + PV$, which dominates phase stability. At lower pressure and higher temperature the entropy term dominates, whereas the PV term becomes more important under high pressure. In the case of a one-component system, the functional dependence of the melting point is easily given by the Clausius–Clapeyron's relation [1]. In this relation, the initial slope of the melting curve depends on the volume and enthalpy change of the system as it undergoes the transformation from solid to liquid states. Because the volume changes of aluminium and germanium at transformation are of opposite sign [17], the melting point of aluminium increases with pressure, whereas that of germanium decreases. In the case of three-phase equilibria on the binary eutectic system, the temperature and composition of the eutectic point shift so as to expand the phase field of the densest phase [1]. Solubility, solidus and liquidus lines and transition points move in the same direction.

As listed in Table III, the molar volumes of fcc, diamond cubic and liquid phases in this system are roughly 10×10^{-6}, 13×10^{-6} and 12×10^{-6} $m^3\,mol^{-1}$, respectively. The fcc phase of aluminium is the densest in the system; the second is the liquid phase, and the third the diamond cubic phase of germanium. The high pressure stabilizes the aluminium phase, the densest phase, at the expense of the less dense liquid and germanium phases, and the eutectic point shifts according to the competition of expansion in the aluminium phase and contraction in the germanium phase. These changes in the phase fields in the Al–Ge system caused by high pressure are in agreement with the generalization that pressure stabilizes the phase of smaller molar volumes.

5. Conclusion

The solidus and solubility lines of aluminium have been determined at 0.1 MPa, 2.2 and 2.6 GPa. The high pressures of 2.2 and 2.6 GPa expand the single-phase field of aluminium by about twice, compared with that at 0.1 MPa. The calculations of the phase diagrams at these pressures are carried out on the basis of thermodynamic and volumetric data at 0.1 MPa. These calculations are in qualitative agreement with the experimental results. The discrepancy

seems to be mainly due to the thermodynamic data at 0.1 MPa.

Acknowledgements

Part of this work was financially supported by Iketani foundation and Japanese Ministry of Education, Science Research fund, Contract number 01 550 551.

References

1. L. KAUFMAN, "Solids under high pressure", edited by W. Paul and D. M. Warschauer (McGraw-Hill, New York, 1963) p. 302.
2. A. J. McALISTER and J. L. MURRAY, "Binary alloy phase diagrams", edited by T. B. Massalski, J. L. Murray, L. H. Bennett and H. Baker, Vol. 1 (American Society for Metals, Metals Park, OH, 1986) p. 116.
3. J. M. CAYWOOD, *Met. Trans.* **4** (1973) 735.
4. V. H. STOEHR and W. KLEMM, *Z. anorg. Allg. Chem.* **241** (1939) 305.
5. S. M. BANOVA, I. A. KORSUNSKAYA, G. M. KUZNETSOV and V. A. SERGEYEV, *Phys. Met. Metall.* **46** (1979) 58.
6. E. YU. TONKOV, "Phase diagrams of elements under high pressure" (Nauk, Moscow, 1979) p. 29.
7. J. B. CLARK and C. W. F. T. PISTORIUS, *J. Less-Common Metals* **34** (1974) 233.
8. A. KINGON and J. B. CLARK, *High Temp.-High Press.* **16** (1984) 137.
9. R. E. HANNEMAN and H. M. STRONG, *J. Appl. Phys.* **36** (1965) 523.
10. T. O. ZIEBOLD and R. E. OGILVIE, *Anal. Chem.* **36** (1964) 322.
11. T. NISHIZAWA and M. HASEBE, *J. Iron Steel Inst. Jpn* **67** (1981) 1887.
12. J. L. MURRAY, "Alloy phase diagrams", edited by L. H. Bennett, T. B. Massalski and B. C. Giessen (North-Holland, New York, 1983) p. 249.
13. I. ANSARA, J. P. BROS and M. GAMBINO, *CALPHAD* **3** (1979) 225.
14. L. KAUFMAN, *ibid.* **3** (1979) 45.
15. D. R. GASKEL, "Introduction to Metallurgical Thermodynamics" (McGraw-Hill, New York, 1973) p. 186.
16. W. B. PEARSON, "Metal physics and physical metallurgy", Vol. 4, edited by G. V. Raynor (Pergamon Press, New York, 1967) p. 313.
17. T. IIDA and R. L. GUTHRIE, "The Physical Properties of Liquid Metals" (Clarendon Press, Oxford, 1988) p. 1.
18. S. P. CLARK Jr, "Handbook of physical constants", Revised Edition (The Geological Society of America, New York, 1966) p. 107.
19. J. R. WILSON, *Met. Rev.* **10** (1965) 558.
20. M. HASEBE and T. NISHIZAWA, *Bull Jpn Inst. Metals* **11** (1972) 879.
21. J. B. CLARK and P. W. RICHTER, *Rev. Phys. Chem. Jpn* **67** (1981) 1887.

Received 6 August 1990
and accepted 12 February 1991